Published in final edited form as:
Biomacromolecules. 2012 June 11; 13(6): 1774–1786. doi:10.1021/bm3002705.

Tuning the Properties of Elastin Mimetic Hybrid Copolymers via a Modular Polymerization Method

Sarah E. Grieshaber[1,$], **Alexandra J. E. Farran**[1,$], **Shi Bai**[2], **Kristi L. Kiick**[1,*], and **Xinqiao Jia**[1,*]

[1]Department of Materials Science and Engineering, Delaware Biotechnology Institute, University of Delaware, Newark, DE 19716

[2]Department of Chemistry and Biochemistry, University of Delaware, Newark, Delaware, 19716

Abstract

We have synthesized elastin mimetic hybrid polymers (EMHPs) via the step-growth polymerization of azide-functionalized poly(ethylene glycol) (PEG) and alkyne-terminated peptide $(AKAAAKA)_2$ (AK2) that is abundant in the crosslinking domains of the natural elastin. [1] The modular nature of our synthesis allows facile adjustment of the peptide sequence to modulate the structural and biological properties of EMHPs. Thus, EMHPs containing cell-binding domains (CBD) were constructed from α,ω-azido-PEG and two types of alkyne-terminated AK2 peptides with sequences of DGRGX$(AKAAAKA)_2$X (AK2-CBD1) and X$(AKAAAKA)_2$XGGRGDSPG (AK2-CBD2, X = propargylglycine) via a step-growth, click coupling reaction. The resultant hybrid copolymers contain an estimated five to seven repeats of PEG and AK2 peptides. The secondary structure of EMHPs is sensitive to the specific sequence of the peptidic building blocks, with CBD-containing EMHPs exhibiting a significant enhancement in the α-helical content as compared to the peptide alone. Elastomeric hydrogels formed by covalent crosslinking of the EMHPs had a compressive modulus of 1.06 ± 0.1MPa. Neonatal human dermal fibroblasts (NHDFs) were able to adhere to the hydrogels within 1 h, and to spread and develop F-actin filaments 24 h post-seeding. NHDF proliferation was only observed on hydrogels containing RGDSP domains, demonstrating the importance of integrin engagement for cell growth and the potential use of these EMHPs as tissue engineering scaffolds. These cell-instructive, hybrid polymers are promising candidates as elastomeric scaffolds for tissue engineering.

Introduction

Elastin is a major extracellular matrix (ECM) protein that provides strength and elasticity to many soft, mechanically active tissues including the skin, lungs, and vocal folds.[2, 3] It is formed by extensive crosslinking of the 72 kDa precursor tropoelastin, which contains hydrophobic, conformationally flexible amino acid domains in alteration with hydrophilic crosslinking domains.[4] We are interested in developing hybrid elastin-mimetic, polymer-peptide hybrid materials that maintain the structural and biological properties of the crosslinking peptide segments in natural elastin, but possess added tunability and chemical diversity imparted by the synthetic polymer domains, and can subsequently be used to form

*To whom correspondence should be addressed: XJ: 302-831-6553 (phone); 302-831-4545 (fax); xjia@udel.edu, KLK: 302-831-0201 (phone); 302-831-4545 (fax); kiick@udel.edu.
$These two authors contributed equally to this work.

Supporting Information Available:
Amino acid analysis of EMHP-CBD2 before and after crosslinking, HPLC analysis of AK2-CBD2, expanded ^{1}H NMR α-CH regions of AK2-CBD2 and EMHP-CBD2, and ^{1}H NMR spectra of AK2-CBD2 and EMHP-CBD2 in DMSO. This material is available free of charge via the Internet at http://pubs.acs.org.

multicomponent hydrogels that can mimic the complex structure of native ECM.[5, 6] Compared to genetically-engineered elastin-like polypeptides (ELPs),[78] the hybrid system is more versatile and easier to produce.[6, 9] Multiblock hybrid copolymers are an attractive intermediary between short peptides and intact ECM proteins. When properly designed, these copolymers can effectively amplify the biological activities of the peptide and elicit highly coordinated and dynamic interactions with the cells.

We have previously reported the synthesis of elastin-mimetic hybrid polymers (EMHPs) with alternating multiblock architecture by a step-growth polymerization method.[1] Specifically, multiblock EMHPs containing flexible synthetic segments based on PEG alternating with alanine-rich, lysine-containing peptides were synthesized by step-growth polymerization using α,ω-azido PEG and alkyne-terminated $(AKAAAKA)_2$ (AK2, A: alanine; K: lysine) peptide, employing orthogonal click chemistry. This modular synthetic approach allows facile substitution of the polymer and peptide components to incorporate desired chemical functionality and structural, mechanical, or biological properties. The crosslinked EMHPs (xEMHPs) exhibited elastomeric properties and had minimal cytotoxicity when cultured in the presence of porcine vocal fold fibroblasts. However, the absence of cell-binding domains (CBDs) in the parent EMHPs limits their utility in tissue engineering applications.

RGD-containing peptides have been widely used to promote cell adhesion on synthetic polymer hydrogels, polysaccharide hydrogels, or other peptide- or protein-based materials that are not naturally cell-adhesive.[10, 11] The RGD sequence is recognized by about half of the known integrins,[12] and is therefore broadly useful for improving cell adhesion. However, modification of the peptide sequence in a multiblock hybrid copolymer can cause significant changes or enhancements in secondary structure, specifically α-helicity, due to interactions between the peptide and polymer components. It has been reported that the covalent attachment of PEG can result in helix stabilization of polymer-peptide conjugates[13, 14] or multiblock hybrid copolymers[15] that contain lysine or arginine. Thus, the secondary structure and the bioactivity of the multiblock hybrid copolymers are likely to be dependent on the composition and the sequence of the peptidic building blocks. While increase in α-helicity is desirable in certain applications, it is important to understand that drastic changes or enhancements in secondary structure could potentially affect mechanical properties and cellular responses.

In this work, EMHPs were synthesized with regularly spaced CBDs as side chains on the multiblock polymers. Two types of CBD-containing EMHPs (EMHP-CBD1 and EMHP-CBD2) were synthesized using telechelic azido-PEG and peptides with a sequence of $DGRGX(AKAAAKA)_2X$ (AK2-CBD1) and $X(AKAAAKA)_2XGGRGDSPG$ (AK2-CBD2, X = Propargylglycine) as the building blocks. The resultant hybrid multiblock copolymers were characterized in terms of their molecular weight, chemical composition and secondary structure. Covalent crosslinking of the multiblock copolymers resulted in elastomeric hydrogels and the ability of these hydrogels to support the attachment and proliferation of dermal fibroblasts was analyzed.

Experimental Section

Materials

All chemicals were used as received without further purification unless otherwise specified. Water was deionized and filtered through a Barnstead NANOpure Diamond water purification system.

Characterization

^{1}H NMR spectra were recorded in D_2O or DMSO-d_6 on a Bruker Avance 400 MHz or Avance 600 MHz NMR spectrometer and the acquired NMR data were analyzed with Bruker Topspin software. Chemical shift values were referenced using the solvent peak at 4.80 ppm (D_2O) or 2.50 ppm (DMSO). The water signal was suppressed by a pre-saturation scheme for all spectra in D_2O.[16, 17] ^{1}H chemical shift assignments of EMHP-CDB1 and EMHPCDB2 were made through a number of 2D-TOCSY spectra at different mixing times (data not shown). FT-IR spectra were obtained with a Thermo Nicolet Nexus 670 spectrometer equipped with a DuraSampIIR II ATR accessory (SensIR Technologies). An average of 128 scans were collected for the background of the clean silicon crystal at a resolution of 4 cm^{-1} from 650 to 4000 cm^{-1}. Polymer and peptide samples were analyzed using the same measurement parameters after depositing the solid material on the silicon ATR crystal and gently pressed during the measurement. The background was automatically subtracted from all sample spectra using the OMNIC software. Gel permeation chromatography (GPC) was conducted on a system comprising a Waters 515 HPLC pump, Ultrahydrogel 250 and Linear (7.8 × 300 mm) columns in series, and Waters 2414 refractive index and 2996 photodiode array detectors. All samples were dissolved at a concentration of about 1–2 mg/mL in 10 mM phosphate buffered saline (PBS) at pH 7.4 and filtered with 0.22 μm PVDF syringe filters before analysis. PBS was used as the mobile phase, and samples were run at a flow rate of 1 mL/min. Molecular weight calibration was based on standards of alkyne-functionalized peptide starting materials and proteins of known molecular weights (myoglobin and catalase, purchased from Sigma-Aldrich), and data was analyzed with Waters Empower software. Amino acid analysis (AAA) was conducted by the Molecular Structure Facility at the University of California, Davis (Davis, CA) using a Hitachi L-8800 sodium citrate-based amino acid analyzer (Tokyo, Japan). Peptide and multiblock copolymer samples were cleaved by HCl hydrolysis, separated with ion-exchange chromatography, and detected using a ninhydrin reaction. ESI-MS was conducted on a Thermo Finnegan LCQ Advantage mass spectrometer with Surveyor MS pump. Samples were dissolved in a mixture of 90/10 methanol/water at a concentration of ca. 0.2 mg/mL and analyzed in a positive ion mode. Peptides were analyzed by reverse-phase high performance liquid chromatography (HPLC) on a Waters Delta 600 (Waters Corporation, Milford, MA) system with a Waters Symmetry 300 C18 analytical column (3 μm particle size, 4.6 × 75 mm), and Waters 2996 photodiode array detector. Semi-preparative scale HPLC purification was conducted with a Waters Symmetry 300 C18 column (5 μm particle size, 19 × 150 mm) and Waters Fraction Collector III.

Synthesis of N_3-PEG-N_3

The hydroxyl end groups of PEG (Acros, M_n = 1450 g/mol) were converted to azide end groups (N_3-PEG-N_3) via a mesylate intermediate, as previously reported.[1] The resultant N_3-PEG-N_3 had an end-group functionality of 96%, as confirmed by ^{1}H NMR.

Synthesis of AK2-CBD1 and AK2-CBD2 Peptides

All peptides were synthesized by standard Fmoc-based solid phase peptide synthesis (SPPS) on a PS3 automated peptide synthesizer (Protein Technologies, Inc., Tucson, AZ). The peptide sequences were $X(AKA_3KA)_2X$ (AK2), $DGRGX(AKA_3KA)_2X$ (AK2-CBD1), and $X(AKA_3KA)_2XGGRGDSPG$ (AK2-CBD2), where A = alanine, K = lysine, R = arginine, D = aspartic acid, G = glycine, S = serine, and P = proline (Protein Technologies, Inc.), and X = propargylglycine (AnaSpec, Fremont, CA). All peptides were synthesized on Rink Amide MBHA resin (Novabiochem, San Diego, CA), and the N-terminus was acetylated by capping with acetic anhydride. The peptides were cleaved and deprotected in trifluoroacetic acid/water/triisopropylsilane (95/2.5/2.5 v/v) for 4–6 h, precipitated twice into cold diethyl ether, collected by centrifugation, then dissolved in water and lyophilized. Characterization

of CBD-free AK2 was reported previously.[1] The crude peptide AK2-CBD1 (yield: 51%) was purified via semi-preparative HPLC (Figure S1) with fraction collection. The mass was confirmed via ESI mass spectrometry (m/z) 1857.7 [$(M+H)^+$, calculated 1858.0]. The AK2-CBD2 peptide was synthesized at a yield of 71% and its mass was confirmed via ESI mass spectrometry (m/z) 1079.5 [$(M+H)^{2+}$, calculated 1079.63], 719.8 [$(M+H)^{3+}$, calculated 720.1]. ^{1}H NMR (D_2O) δ (ppm): 3.95–4.53 (m, 24H, NH-C***H***-CO), 3.85 (m, 2H, Ser C***H*****$_2$**-OH), 3.75 (m, 2H, Pro C***H*****$_2$**-NH-), 3.22 (m, 2H, Arg C***H*****$_2$**-NH-C(NH_2)=NH_2^+), 3.02 (m, 8H, Lys C***H*****$_2$**NH_2), 2.73–2.84 (m, 6H, Asp C***H*****$_2$**-COOH and PrGly C***H*****$_2$**C ≡ CH), 2.48 (m, 2H, PrGly CH_2C ≡ C***H***), 2.32 (m, 3H, terminal COC***H*****$_3$**), 1.9–2.07 (m, 6H, Pro CHC***H*****$_2$**C***H*****$_2$**CH_2-NH- and CHC***H*****$_2$**$CH_2CH_2CH_2NH_2$), 1.68–1.84 (m, 22H, Arg C***H*****$_2$**C***H*****$_2$**CH_2-NH-C(NH_2)=NH_2^+ and Lys CHC***H*****$_2$**CH_2C***H*****$_2$**CH_2NH_2), 1.41 (m, 38H, Ala CHC***H*****$_3$** and Lys $CHCH_2$C***H*****$_2$**$CH_2CH_2NH_2$)

Synthesis of CBD-containing Multiblock Hybrid Copolymers (EMHPs)

CBD-containing EHMPs were synthesized using N_3-PEG-N_3 and AK2-CBD1 or AK2-CBD2 and the resultant hybrid copolymers are referred to as EMHP-CBD1 and EMHP-CBD2, respectively. In a typical procedure, N_3-PEG-N_3 and the AK2-CBD1 or AK2-CBD2 peptide were dissolved at concentrations of 18–20 mM each at a molar ratio of 1:1 in a mixture of water/DMSO (80/20 v/v), $CuSO_4 \cdot 5H_2O$ (0.2 eq, based on molar concentration of alkyne groups), sodium ascorbate (1 eq), and the ligand tris-(benzyl-triazolylmethyl)amine (TBTA, synthesized following a previously reported method[1, 18]) (0.4 eq). The reaction mixture was stirred at 80 °C for 24 h, then diluted with water and stirred at room temperature in the presence of Cuprisorb resin (Seachem Laboratories, Madison, GA) for another 24 h to remove residual copper. The resin was removed by vacuum filtration. The yellow filtrate was collected, dialyzed against water at room temperature (MWCO 3500) for 3 days, then lyophilized to obtain the CBD-containing EMHP as a fluffy, pale yellow solid. Yield: 40%. ^{1}H NMR of EMHP-CBD1 (D_2O) δ (ppm): 7.94 (s, 3H, triazole C=C***H***), 4.65 (m, 3H, linker triazole-propargylglycine NH-C***H***-CO), 3.96–4.57 (m, 15H, NH-C***H***-CO), 3.71–3.83 (m, 99H, OC***H*****$_2$**C***H*****$_2$**), 3.22-3.02 (m, 12H, Arg C***H*****$_2$**-NH-C(NH_2)=NH_2^+ Lys C***H*****$_2$**NH_2, Asp C***H*****$_2$**-COOH), 2.06-1.84 (m, 18H, Arg C***H*****$_2$**C***H*****$_2$**CH_2-NH-C(NH_2)=NH_2^+ and Lys CHC***H*****$_2$**CH_2C***H*****$_2$**CH_2NH_2), 1.41 (m, 30H, Ala CHC***H*****$_3$** and Lys $CHCH_2$C***H*****$_2$**$CH_2CH_2NH_2$). ^{1}H NMR of EMHP-CBD2 (D_2O) δ (ppm): 7.94 (s, 1H, triazole C=C***H***), 4.65 (m, 3H, linker triazole-propargylglycine NH-C***H***-CO), 3.96–4.57 (m, 24H, NH-C***H***-CO), 3.71–3.83 (m, 218H, OC***H*****$_2$**C***H*****$_2$**), 3.22 (m, 2H, Arg C***H*****$_2$**-NH-C(NH_2)=NH_2^+), 3.02 (m, 8H, Lys C***H*****$_2$**NH_2), 2.63–2.68 (m, 2H, Asp C***H*****$_2$**-COOH), 2.32 (m, 3H, terminal COC***H*****$_3$**), 2.0 (m, 4H, Pro CHC***H*****$_2$**C***H*****$_2$**CH_2-NH-), 1.68–1.84 (m, 20H, Arg C***H*****$_2$**C***H*****$_2$**CH_2-NH-C(NH_2)=NH_2^+ and Lys CHC***H*****$_2$**CH_2C***H*****$_2$**CH_2NH_2), 1.41 (m, 38H, Ala CHC***H*****$_3$** and Lys $CHCH_2$C***H*****$_2$**$CH_2CH_2NH_2$).

Covalent Crosslinking

EMHPs were crosslinked by adding hexamethylene diisocyanate (HMDI, Sigma Aldrich) to a 10 wt% solution of EMHP or EMHP-CBD2 dissolved in DMSO. The ratio of EMHP to HMDI was 1:2 (w/v), which was calculated to be a molar ratio of approximately 15:1 isocyanate:lysine functional groups. After vortex mixing, ~100 μL of the EMHP/HMDI solution was added to a 1 mL syringe, covered, and allowed to crosslink overnight at room temperature. The crosslinked gels (xEMHP, or xEMHP-CBD2) were subsequently dried in an oven at 50–60 °C for 8–10 h. After removal from the syringes, the gels were soaked in acetone for 2 h followed by DI water for at least 24 h until immediately before the measurement.

Mechanical Testing

Mechanical analysis was conducted on an RSA III dynamic mechanical analyzer (TA Instruments, New Castle, DE) using an 8 mm parallel plate geometry. Ten cyclic loading and unloading tests were conducted on each sample at a compression rate of 0.05 mm/s. The samples were allowed to recover for approximately 1 min between cycles. The compressive modulus was calculated using the linear portion of the stress-strain curve between 5 and 10% strain, and is reported as an average of 8 individual samples ± the standard deviation.

Water Uptake

EMHP-CBD2 gels (10 repeats) were prepared as described above. After soaking in acetone and water to remove residual or uncrosslinked material, pieces of gel were dried under vacuum overnight before recording the dry weight. The samples were then immersed in water for 24 h at room temperature. The wet weights were measured after blotting excess water, and the swelling ratio was calculated as the wet weight divided by the dry weight for each sample. The data reported were an average of at least three separate repeats ± the standard deviation.

MTT Assay

Neonatal Human Dermal Fibroblasts (NHDFs) (ATCC, Manassas, VA) were cultured in fibroblast basal media (ATCC) supplemented with recombinant human fibroblast growth factor beta (rhFGF-β), L-glutamine, ascorbic acid, hydrocortisone hemisuccinate, recombinant human insulin, 2% fetal bovine serum (FBS), and penicillin (10 units/mL), streptomycin (10 μg/mL), and amphotericin B (25 ng/mL) (ATCC). Confluent cells (passage 3) were trypsinized and seeded onto 24-well plates at a density of 10,000 cells/well in 1 mL of cell culture media. The sterile-filtered (0.22 μm) peptide and polymer solutions (N_3-PEG-N_3, AK2- CBD2, and EMHP-CBD2) were added to each well so that their final concentrations were in the range of 0.002–2.00 mg/mL. The relative toxicity of these materials was assessed with an MTT cell proliferation assay kit (ATCC) after 3 days of culture without changing the medium. The absorbance was measured at 590 nm with a plate reader (Perkin Elmer Universal Microplate Analyzer). Cells cultured under the same conditions in pure medium were used as a positive control, and the results were expressed as the measured absorbance normalized to that of the controls. The data reported were an average of five separate repeats ± the standard deviation. Statistical analysis was performed using a two-tailed, equal variance Student's *t-test*, where a *p*-value of ≤0.02 was considered to be statistically different.

Cell Attachment

EMHP/HMDI solutions were prepared in DMSO as described above. EMHP hydrogel films were prepared by adding 2 μL drops of solution onto glass coverslips (Fisher). The crosslinking reaction was allowed to occur overnight at room temperature while the solvent slowly evaporated. The dry films were subsequently immersed in acetone for 2 h, soaked in water for at least 2 h, and allowed to dry again at room temperature. The hydrogel-coated glass coverslips and blank glass coverslip controls were sterilized with 70% ethanol for 20 minutes under the UV light (254 nm), and then left to dry under the UV light for 20 min. Samples were rehydrated overnight in NHDF media that was free of phenol red and FBS. The next day, media were removed before cell seeding. Cell attachment and morphology were assessed fluorescently by labeling NHDFs pre- or post-seeding.

Cell tracker staining—NHDFs (passage 3) were pre-stained with CellTracker™ Green (5-chloromethylfluorescein diacetate, Invitrogen) according to the manufacturer's instructions. The stained cells were trypsinized, counted and re-suspended in phenol red and

FBS-free media at a concentration of 500,000 cells/mL A 25 μL of cell suspension was then deposited on the gelcoated coverslips (films of approximately 5 mm diameter) at a density of 62,500 cells/cm^2, and the cells were incubated for 3 h at 37 °C with 5% CO_2. Samples were then rinsed with PBS, fixed with 4% paraformaldehyde (Electron Microscopy Science, Hatfield PA) for 15 min, and rinsed again with PBS before being imaged with a confocal microscope (Axiovert LSM 510, Zeiss).

F-actin/Vinculin staining—NHDFs (passage 3) were trypsinized, counted, and re-suspended in phenol red- and FBS-free media at a concentration of 100,000 cells/mL. A 25 μL drop of the cell suspension was deposited on top of each gel sample. After 1 h incubation, samples were either subjected to immunostaining (1 h time point) or replenished with 1 mL of fresh media for additional culture for 24 h. At a pre-determined time, samples were rinsed with 1 mL PBS, fixed with 4% paraformaldehyde in PBS for 15 min, permeabilized for 5 min with 0.1% Triton-X100 in PBS, and blocked for 2 h with 3% BSA (bovine serum albumin, Jackson ImmunoResearch, West Grove PA) in PBS. Following blocking, samples were incubated for 1 h with mouse antivinculin (1/100 in 3% BSA, Millipore, Billerica MA), then incubated for 1 h with Alexa 488 anti-mouse (1/100 in 3% BSA, Invitrogen), and TRITC-phalloidin (1/200 in 3% BSA, Millipore) and finally counterstained with Draq5™ (1/1000, Axxora). Between each step, samples were rinsed 2 or 3 times with a washing buffer (0.05% Tween-20 in PBS, Fisher). Before imaging, samples were mounted using Fluoro Gel mounting medium (Electron Microscopy Science). Imaging was done using a Zeiss LSM 510 confocal microscope.

Cell Proliferation

EMHP solutions containing HMDI were prepared in DMSO as described above. To prepare the gel samples, 70 μL of solution was added to a cylindrical glass well (9 mm I.D., 11 mm O.D., surface area ~0.635 cm^2) to obtain a hydrogel sample with a thickness of ~1 mm. At least three samples were prepared for every time point in each experiment. The wells were covered with a glass slide and the gels were allowed to crosslink overnight at room temperature. On the following day, the crosslinked gels and blank glass wells were soaked in large volumes (at least 300 mL) of acetone for 2 h, then soaked in large volumes of DI water for at least 24 h (changing water once) until the start of the experiment. The gels were sterilized and equilibrated in serum free NHDF media following the procedure described above. The trypsinized NHDFs (passage 3) were suspended in phenol red- and FBS-free media at a concentration of 100,000 cells/mL and a 200 μL cell suspension was added to each gel. After 6, 24, 48, 72, and 168 h, cells were rinsed with 200 μL PBS. Dead cells were removed by the rinsing procedure, and the remaining attached cells were trypsinized for 5 min, and counted with a hemacytometer. The counting procedure was repeated 3 times and the experiment itself was repeated 3 times. The results were expressed as mean ± SEM and statistical analysis was conducted using a two-tailed, equal variance Student's *t-test*, where a *p*-value of ≤0.01 was considered to be statistically different.

Results and Discussion

Elastin mimetic hybrid polymers (EMHPs) with a strictly alternating molecular architecture were previously synthesized using copper (I)-catalyzed azide-alkyne cycloaddition (CuAAC) as a step-growth polymerization method using telechelic, azide-functional PEG and an alkyne-terminated peptide that is abundant in the crosslinking domains of natural elastin. [1] The EMHPs were found to have mechanical properties similar to the native elastin, but lacked cell-binding motifs. Although tropoelastin does not contain an RGD motif, cell adhesion to tropoelastin is integrin-mediated. In a recent study, the C-terminal GRKRK motif of tropoelastin has been identified as the integrin binding motif and integrin $\alpha_V\beta_3$ as

the major receptor necessary for fibroblast adherence and spreading onto human tropoelastin.[19] In this proof-of-concept investigation, we employed well-established cell-binding domains (CBDs) containing the RGD sequence to demonstrate the modular nature of our system that allows for ready incorporation of biologically active peptide motifs. We also demonstrated that depending on the specific amino acid sequence, in some cases these motifs could significantly increase the helicity of the EMHPs through H-bonding interactions between the PEG and peptide. Careful selection and strategic placement of CBDs in the AK2 peptide led to the production of xEMHPs with the ability to support the attachment and proliferation of dermal fibroblasts.

Synthesis of CBD-containing EMHP

CBD-tagged AK2 peptides were synthesized by standard Fmoc SPPS protocols. The peptide design was based on the AKA_3KA crosslinking domains from tropoelastin, with the alkyne-containing non-natural amino acid propargylglycine (denoted as X) at either end of the peptide for CuAAC reaction with the azide-functional synthetic polymer domains. Although about half of the 24 known integrins, including $\alpha_v\beta_3$, $\alpha_5\beta_1$, and $\alpha_{IIb}\beta_3$, bind RGD ligands, the amino acids adjacent to the RGD sequence affect which integrins bind most readily.[20] The AK2-CBD1 peptide is included to demonstrate the effect of these additional peptide sequences on the structural properties of the multiblock polymers. Cyclic DGR peptides were recently shown to selectively bind the $\alpha_v\beta_5$ integrin,[21] and other DGR-containing peptide sequences were able to specifically bind bladder tumor cells.[22] While some competitive binding studies have indicated that DGR-containing peptides have significantly lower integrin binding activity than RGD-containing peptides,[23, 24] in other cases, the binding activity of DGR was observed to be as high as RGD in inhibiting cell attachment to fibronectin.[25] The RGDSP sequence in AK2-CBD2 was selected to promote cell adhesion via the $\alpha_5\beta_1$ integrin, and adding flanking amino acids has been shown to increase the peptide activity compared to RGD alone.[20, 26]

In both AK2-CBD1 and AK2-CBD2 peptides, glycine residues were introduced as flexible spacers. The CBDs were also placed outside the propargylglycine residues so that after polymerization by CuAAC, the cell adhesion domains would appear as side chains along the multiblock polymer backbone for greater accessibility to integrins on the cell surface. For human mesenchymal stem cells encapsulated in PEG hydrogels, RGD sequences tethered by one terminus to the gels resulted in a greater number of focal adhesions compared to gels that contained RGD sequences attached to the gel through both termini of the peptide.[27] Steric hindrance was proposed to cause more difficulty in integrin binding to the RGD tethered at both termini, and an RGD sequence along the backbone of multiblock polymers in a crosslinked hydrogel would be similarly confined and hindered. Separately, azide-functional PEG (M_n=1450 g/mol) was synthesized according to the previously reported method via mesylation of the PEG hydroxyl end groups followed by a substitution reaction with sodium azide. The azide end group functionality was calculated as 96% by NMR.[1]

The step-growth CuAAC polymerization reactions between N_3-PEG-N_3 and alkynefunctional AK2-CBD1 and AK2-CBD2 peptides are shown in Scheme 1A and B, respectively. If the copper catalyst and the ligand are chosen properly, the CuAAC reaction can be conducted in a wide variety of organic and aqueous solvents.[1, 28, 29] In this case, a mixture of 80/20 water/DMSO was chosen for optimum solubility of all reagents. The reaction is also highly selective and can be conducted in the presence of a number of other chemically reactive functional groups, including those present on the side chains of the various amino acids in the AK2-CBD2 peptide domains. CuAAC reactions have been conducted in the presence of RGD sequences as well as lysine residues without the occurrence of side reactions.[30, 31] In addition, the 1,2,3 triazole ring products are good

peptide bond mimics because they are planar, possess a dipole moment, and the nitrogen atoms can participate in H-bonding with peptide amide NH groups.[32, 33]

The step-growth polymerization was successful with the both AK2-CBD1 and AK2-CBD2 peptides and the unreacted peptide and PEG monomers were removed by extensive dialysis. A molecular weight increase was observed for the AK2-CBD1 peptide (M_n = 1,858 g/mol) upon conversion to the EMHP-CBD1 product (Figure 1A, M_n = 14,800 g/mol; M_w = 51,600 g/mol, calculated from protein standards). The molecular weight was estimated to correspond to an average of seven to ten total polymer and peptide blocks per chain, with a maximum of up to twenty five blocks. A molecular weight increase was also observed for the AK2-CBD2 peptide starting material (M_n = 2,155 g/mol) upon conversion to the EMHP-CBD2 product (Figure 1B, M_n = 13,180 g/mol; M_w = 31,700 g/mol), and the molecular weight was estimated to correspond to an average of five to seven total polymer and peptide blocks per chain, with a maximum of up to fifteen blocks. The molecular weight is lower for EMHP-CBD2 possibly due to the steric hindrance of the longer GGRGDSPG sequence which could impede the reaction of the alkyne groups with PEG diazide. The inherent step-growth nature of the polymerization inevitably gave rise to hybrid copolymers of varying sizes.[34] Consequently the GPC trace showed a relatively broad and multimodal molecular weight distribution. A slower reaction and lower molecular weight could explain the lower polydispersity index (PDI) observed for EMHP-CBD2 (PDI=2.4) compared to EMHP-CBD1 (PDI=3.5)

FTIR and NMR studies were conducted to confirm the successful synthesis of the CBD-containing AK2-CBD2 peptide and EMHP-CBD2. FTIR (Figure 2) confirmed the presence of both PEG (C-O stretch at 1100 cm^{-1}) and peptide (N-H stretch at 3,280 cm^{-1}, Amide I at 1,650 cm^{-1}, and Amide II at 1,530 cm^{-1}) bands in the EMHP-CBD2 product. After the polymerization, the azide asymmetric stretch at 2,100 cm^{-1} in the N_3-PEG-N_3 starting material had mostly disappeared (some azide groups remain as end groups on the EMHP), further indicating the high efficiency of the coupling reaction. From estimation of the areas of the azide bands in the PEG starting material and EMHP-CBD2, relative to the C-O bands, approximately 30% of the azide peak remained after the reaction. This agrees with the GPC results as it corresponds to an average of about five to seven total blocks per chain if three or four PEG blocks were in alteration with peptide blocks and two (of the six or eight total) PEG azide end groups were left unreacted. It is possible that the presence of lower molecular weight products or unreacted PEG diazide may also increase the area of the residual azide peak. The remaining azide end groups could potentially be useful for further modification of the EMHPs with alkyne-functional biomolecules.

The ^{1}H NMR spectra of the AK2-CBD2 peptide and EMHP-CBD2 are shown in Figure 3A and 3B, respectively. In the EMHP-CBD2 spectrum (Figure 3B), a peak from the triazole ring (a: C***H***) formed as a result of the CuAAC reaction is clearly visible at 7.9 ppm. An intense peak from the PEG repeat unit (b: C$\boldsymbol{H_2}$O at 3.7 ppm) and several peptide peaks including the lysine side chain (c: C$\boldsymbol{H_2}$$NH_2$ at 3.0 ppm) are also apparent. The peptide peaks are broader in the EMHP-CBD2 spectrum because their mobility is more restricted in the multiblock polymer. The NMR results further confirm the successful synthesis of CBD-containing EMHPs.

Secondary structure of CBD-containing EMHP

The secondary structures of the peptide and EMHP were monitored by ^{1}H NMR and CD spectroscopy. As shown in the CD spectrum of AK2-CBD1 (Figures 4A), the peptide alone exhibited α-helical conformation, as evidenced by minima at 208 and 222 nm. The fractional helicity was calculated from the ratio of the mean residue ellipticity at 222 nm ($[\theta]_{222}$) over the theoretical value for a 100% helical peptide $[\theta]_n$), adjusted to account for

the peptide length,[35] and the results are summarized in Table 1. Previously, the AK2 (CBD-free) peptide alone was shown to have increased helicity when the pH was raised because of decreased charge repulsion upon deprotonation of the lysine residues, but the helicity of the AK2 domain in the EMHP was significantly reduced and was not responsive to pH,[1] which was attributed to the hydrophilicity and steric hindrance of the PEG segments. A pH effect similar to that previously observed for the AK2 peptide was observed for the AK2-CBD1 peptide (Figure 4A). At pH 7.4, AK2-CBD1 had a higher fractional helicity (9.3%) than the AK2 peptide (6.3%). When the pH was raised to 12, the helicity of AK2-CBD1 increased to 13.7%, which is slightly lower than the AK2 peptide alone without any side chains (15.8% at pH 11.9). Remarkably, for EMHP-CBD1 (Figure 4B), the helicity was amplified to 42.4% at pH 7.4, and increased only slightly further upon deprotonation of the lysine residues (46.1% at pH 12). We speculate that reduced electrostatic repulsion and increased helix stabilization, due to H-bonding of the guanidinium groups of the arginine residues (and amine groups of the lysine residues, to a lesser extent) with the oxygen atoms in PEG (as well as the peptide backbone carbonyl groups), may be the reason for this effect. Arginine can form up to five H-bonds with oxygen, and has been found to play an important structural role in proteins such as carbonic anhydrase, xylose isomerase, and ribulose-l,5-bisphosphate carboxylase/oxygenase.[36] In a related work, arginine-rich coiled-coil-forming peptides also showed an increase in helical content upon formation of multiblock copolymers of the peptides with PEG.[15] As mentioned previously, the triazole rings can also participate in H-bonding either through the nitrogen atoms bonding with peptide backbone amide NH groups, or the CH groups bonding with carbonyl oxygens,[33] and these interactions may further stabilize the helices. The AK2-CBD2 peptide alone, in contrast, exhibited reduced helicity as compared to the CBD-free AK2 peptide, and was significantly lower at pH 12 when the lysine amines were deprotonated (7.8% for AK2-CBD2 compared with 15.8% for AK2) (Figure 4C). The GGRGDSPG sequence in the AK2-CBD2 peptide may introduce steric hindrance and result in a lower percent helicity than the CBD-free peptide, even when the lysine residues are uncharged. As observed for EMHP-CBD1, however, the helicity of the peptides in the EMHP-CBD2 was greater than that of the peptide alone at all pH values from 7.4 to 12. This effect is also likely due to H-bonding interactions between arginine and the PEG oxygen atoms. However, in the case of EMHPCBD2, the helicity does not increase as dramatically (Figure 4D) compared to the peptide starting material (Figure 4C), perhaps because the longer side chain may hinder the formation of H-bonds between PEG and the arginine or lysine residues.

These results indicate two salient features relevant for the application of these types of polymers as elastomeric substrates for cells. First, the EMHP-CBD1 data demonstrate that the composition of the peptide can drastically affect the secondary structure of the peptide in the context of multiblock polymers, which may be a useful structural handle in future studies should increased helicity of the peptide segments result in variation of the properties of the EMHPs. However, when considering availability of the peptides for integrin binding, minimal extent of such H-bonding would be desirable. At pH 7.4, the high helicity of the EMHP-CBD1 may indicate that a large percentage of the arginine residues would be engaged in H-bonding and not available for integrin binding. Given the lower helicity of the EMHP-CBD2 constructs, all subsequent studies were conducted using only the AK2-CBD2 peptide and EMHP-CBD2.

When comparing the expanded ^{1}H NMR spectrum of the AK2-CBD2 peptide alone with that of the EMHP-CBD2 in the region of the peptide α-CH groups along the backbone (4.1–5.0 ppm) (Figure S2A and S2B), we noticed that the peaks in the EMHP spectrum were shifted upfield from their original positions in the peptide spectrum. The ^{1}H NMR chemical shifts of the α-CH for each amino acid have been reported to shift upfield upon α-helix formation and downfield upon β-sheet formation, relative to the values reported for random

coil conformations.[37–39] As shown in Figure S2A and S2B, the α-protons of serine and proline at approximately 4.53 and 4.45 ppm in the AK2-CBD2 peptide shifted upfield to 4.44 and 4.38 ppm respectively, in EMHP-CBD2. The overlapping arginine and lysine alpha proton peaks at ~4.35 ppm have most likely been shifted upfield as well, merging with the alanine α-CH peak centered around 4.28 ppm in the peptide spectrum and increasing the area of the alanine α-CH peak. These peak shifts suggest the formation of α-helical structures in the multiblock copolymers. Due to the relatively short length of the peptide segments in EMHPs, the observed shifts are not as large as the average shift reported for larger proteins with a higher α-helical content.[37] The peak at 4.61 ppm does not appear in the spectrum of the peptide, as it results from the α-protons of the propargyl glycine residues after the CuAAc reaction. The high concentration of the NMR samples (approximately 20 times higher than the concentration of the CD samples) may also contribute to the observed helix stabilization through increased H-bonding. The ^{1}H NMR spectra of the AK2-CBD2 peptide and the resultant EMHP were also studied in DMSO (Figure S3) to assess the conformations of the peptide domains under conditions more similar to those used during the crosslinking reaction. Similar upfield shifts of the alpha protons were observed, indicating that the peptide domains are also helical in DMSO (Figures S3A–D).

Hydrogel Characterization

The CBD-containing EMHPs were crosslinked with HMDI via the reaction between the isocyanates and the lysine amines. Amino acid analysis was employed to calculate the degree of crosslinking and to confirm that all functional groups in the RGDSP sequence were preserved after crosslinking. The degree of crosslinking was calculated by comparing the lysine content before and after crosslinking.[1, 40] As shown in Table S1, the lysine content was reduced in the crosslinked samples, and comparison of the lysine/alanine ratios before and after crosslinking indicates that approximately 75% of the lysine amines were consumed during crosslinking in the xEMHP-CBD2 hydrogels. The relative ratios of aspartic acid, arginine, and serine (compared to alanine), in contrast, remain constant before and after crosslinking, confirming the expectation that the side-chain functional groups of these amino acids are not chemically modified during the crosslinking reaction. This is in agreement with previous studies conducted on RGD-containing ELPs.[41]

The compressive modulus of xEMHP-CBD2 was measured on a dynamic mechanical analyzer (DMA). Ten compression cycles were collected for each sample, and representative stress-strain curves are shown in Figure 5. Although the samples exhibited some permanent plastic deformation as indicated by the stress returning to zero at about 5% strain, the curves from repeated cycles are perfectly overlapping. The permanent deformation may be caused by irreversible structural changes after compression, as the samples did not fully return to their original shape over extended periods of time. The modulus was calculated to be 1.06 ± 0.1MPa for fully hydrated xEMHP-CBD2 gels, which is in the range of literature values for the modulus of native elastin (0.1–1.2 MPa).[7, 42, 43] The xEMHP-CBD2 hydrogels had a swelling ratio of 4.5 ± 1.1, demonstrating that they are able to absorb a significant amount of water.

Cellular Responses

The hybrid multiblock copolymers are designed for use as instructive scaffolds for the engineering of mechanically active tissues. The toxicity of the PEG diazide and AK2-CBD2 peptide starting materials, as well as that of the uncrosslinked EMHP-CBD2, was measured using an MTT assay with neonatal human dermal fibroblasts (NHDFs). The average absorbance shown in Figure 6 was normalized, for all samples, to a positive control of cells in unmodified media. No significant toxicity was observed from AK2-CBD2, N_3-PEG-N_3,

and EMHP-CBD2 at a concentration of 0.002–0.2 mg/mL, despite the positive charge of the AK2-CBD2 peptide.[44] All samples had a normalized absorbance above 0.85 in this concentration range, which is similar to results observed previously with the CBD-free AK2 peptide and EMHP. The toxicity of soluble EMHP-CBD2 at 2 mg/mL was slightly higher than that of the peptide or PEG starting materials, which may be due to a small amount of residual copper bound to the polymer.

The moderate toxicity observed for soluble EMHP-CBD2 at 2 mg/mL does not necessarily translate to the crosslinked hydrogels. Because the lysine amines were utilized for crosslinking purposes, the impact of any residual positive charges would be diminished after the crosslinking reaction. Additional purification processes were applied to the hydrogels, thereby allowing for future removal of toxic impurities (e.g. residual copper) trapped in the polymers. When cultured in a medium containing soluble polymers, cells are in direct contact with all soluble components in the medium. On the other hand, when cultured on the crosslinked hydrogels, cells are only exposed to the surface of the hydrogels, therefore, the overall concentration of the residual copper, if any, detected by the cells would be significantly lower.

We subsequently investigated the ability of the crosslinked, CBD-containing EMHPs to support the attachment and proliferation of NHDFs. To observe cell attachment and growth on xEMHP-CBD2, NHDFs were seeded on the hydrogel surface in serum-free media so that the contribution of the cell adhesion domains could be identified without the interference from serum proteins. Cell attachment after 3 h was observed by using fluorescently labeled cells. As shown in Figure 7, NHDFs attached and spread on the xEMHP hydrogels with (Figure 7C) or without the RGDSP domains (Figure 7B) as well as on the glass control (Figure 7A) within 3 h of culture. It has been documented that fibroblasts can attach to hydrophilic surfaces such as glass even in the absence of serum, and that attachment improves with increased surface wettability or higher surface free energy.[45] Poly(L-lysine) and other positively charged surfaces have also been shown to promote and stabilize fibroblast attachment both in the presence and absence of serum.[46–48] In addition, the adhesion of bone marrow stromal cells was improved and several adhesion genes were up-regulated when the cells were seeded on films of triblock poly(ethylene glycol)-poly(L-lactic acid)-poly(L-lysine) (PEG-PLLA-PLL) compared to films of polymer without PLL, showing the beneficial effect of positive surface charges on cell adhesion.[49] On the xEMHP gels, cell attachment may initially be facilitated by electrostatic interactions between the positively charged lysine residues and negatively charged cell membranes.[50] In human tropoelastin, which does not contain an RGD sequence, the mechanism of cell attachment is also thought to be cation-dependent and involves the C-terminal GRKRK motif.[19]

Cell attachment to ECM ligands is integrin-mediated and involves the formation of focal adhesion complexes.[51] NHDFs seeded on the xEMHP hydrogels were also stained to visualize the cell nuclei, F-actin stress fibers, and vinculin in the formation of focal adhesions after 1 and 24 h (Figure 8). After 1 h, cells had attached to the substrates and cell processes were observed on xEMHP hydrogels with or without RGDSP domains. It should be noted that some staining of the hydrogel background was observed. This background staining may be due to physical interactions of the phalloidin and the vinculin antibody, both of which contain peptide bonds, with the peptide domains of the xEMHP hydrogels. However, in all cases the cells are stained more prominently than the gel background and can be clearly visualized.

After 24 h, NHDF cells had spread out on both EMHP substrates and displayed elongated cell morphology (Figure 8). Cells spread most readily on glass, but filopodia were observed anchoring the cells onto both types of xEMHP gels. The vinculin and F-actin stress fibers

did not appear to be as strongly oriented and polymerized as for cells cultured on glass; this is likely due to the greater degree of surface roughness and the lower modulus of the xEMHP gels (xEMHP: 0.12 MPa;[1] xEMHP-CBD2: 1.06 MPa, see above) compared to glass (~70 GPa).[52, 53] Although the NHDFs were able to attach and spread on both gels, they seemed to elongate slightly more on gels containing the RGDSP domains and to have a shape that is more similar to the cells seeded on glass. It is likely that both integrin engagement and charge-charge interactions contribute to cell attachment on xEMHP-CBD2 hydrogels.

Although both surfaces supported cell adhesion, differences in the proliferation of cells on the xEMHPs was assessed by seeding the crosslinked gels with NHDFs and counting the cells at 6, 24, 48, 72 and 168 h (Figure 9). Six and twenty-four hours post-seeding, no statistical difference in the cell number was observed between the gels with or without RGDSP. However, after 48 h, the cell number on xEMHP-CBD2 was significantly higher than that on xEMHP without integrin-binding domains. Over 7 days of culture, NHDFs were able to proliferate on the xEMHP-CBD2 gels up to a cell number that was 3.6 times higher than the number at 6 h post-seeding. On xEMHP gels, the cell number did not increase significantly from 6 h to 7 days post-seeding. These results indicate that although the initial cell adhesion is similar on both EMHP gels in terms of cell number and shape, specific cell-receptor interactions with the immobilized RGDSP domains are required for cell proliferation to occur on the EMHP hydrogel surface. After 7 days, the fibroblasts will have produced significant amounts of ECM components that may contribute further to cell adhesion and proliferation. However, the presence of integrin-binding RGD domains allows signal transduction and FAK activation, and has been reported to result in the deposition of more organized ECM components, specifically collagen,[54] and the synthesis of more uniform tissue *in vivo*.[55] These factors may also contribute to the increased proliferation observed on xEMHP-CBD2. Noteworthy, NHDFs exhibited a significantly higher proliferation capacity on glass than on xEMHPs with or without RGDSP (Figure 9). This is not surprising considering the higher modulus of the glass substrate compared to xEMHPs.[53, 56] Additionally the better cell attachment on glass led to a higher initial seeding density which in turn promoted a faster cell proliferation.

Similar cell adhesion and proliferation results to the xEMHP and xEMHP-CBD2 gels were observed on a poly(D,L-lactic-co-glycolic acid) (PLGA) mesh functionalized with both amine groups and a covalently grafted RGD peptide.[57] The aminated PLGA mesh showed improved cell attachment compared with the original PLGA mesh because of the positively charged amine groups, but cell adhesion and proliferation were further enhanced when the PLGA was both aminated and modified with the RGD-labeled peptides. As in the xEMHP-CBD2 gels, the PLGA meshes also contained PEG, but the non-adhesive effect of the PEG was overwhelmed by the positively charged amine groups as well as the RGD cell adhesion domains. These results, along with the results observed from the xEMHP hydrogels, demonstrate that initial cell adhesion can be achieved through electrostatic interactions, but the presence of integrin-binding domains is critical for cell proliferation.

The number of integrin-binding domains required for cell adhesion, spreading, and proliferation has been studied on a variety of substrates, and the RGDSP density on the surface of the xEMHP-CBD2 hydrogels was estimated for comparison with previous literature values. When considering a 10 nm hydrogel surface layer exposed to cells (in wells of the same diameter used in the proliferation studies, see Figure 9 and related description), the density of RGDSP on the xEMHP-CBD2 hydrogel surface can be calculated as approximately 26 nmol/cm^2 based on a concentration of 10 wt% polymer, the known molecular weight of the soluble EMHP as determined by GPC (Figure 1), and the assumption that all multiblock copolymer chains contain strictly alternating polymer and

peptide blocks (therefore the chains can be estimated to contain an average of three RGDSP peptide units). Human foreskin fibroblasts were shown to attach and spread on glass with covalently immobilized GRGDY peptides at a surface concentration of 1 fmol/cm^2, but at least 10 fmol/cm^2 was required for focal contact and stress fiber formation.[58] On alginate gels containing GGGGRGDY peptides, myoblasts were able to attach at a surface concentration of 1 fmol/cm^2, but a higher density of 10 fmol/cm^2 was required for significant spreading, and optimum proliferation was achieved at 30 fmol/cm^2.[59] Although the RGDSP surface density in the xEMHP-CBD2 hydrogels is higher than these values, the concentration employed here may be necessary to account for the fact that not all of the RGDSP units may be accessible to cells due to the linker length, surface roughness of the hydrogels, and H-bonding of a number of the arginine residues with the PEG backbone as described above.

Conclusions

Multiblock EMHPs were synthesized by a step-growth, click coupling of α,ω-azido PEG and alkyne-terminated peptides with a sequence of DGRGX(AKAAAKA)$_2$X (AK2-CBD1) and X(AKAAAKA)$_2$XGGRGDSPG (AK2-CBD2). The CBD-containing EMHPs exhibited increased helical structure compared to the peptides alone, likely owing to H-bonding between the arginine residues with the oxygen atoms in PEG. EMHP-CBD2 was crosslinked into hybrid hydrogels that had a compressive modulus in the same range as native elastin. Neonatal human dermal fibroblasts were able to attach to the EMHP hydrogels 1 h post seeding, and adopt a spindleshaped morphology after 24 h of culture. Initial cell adhesion is most likely due to the interaction of positively charged lysine and arginine residues with the cell membrane in addition to integrin engagement through the RGDSP domains. However, after 7 days, the cell number increased only on the RGDSP-containing EMHPs, showing that the integrin-binding domains are needed for proliferation. The CBD-containing EMHPs are promising tissue engineering scaffolds that are not only strong and elastic, but can support cell adhesion and growth.

Supplementary Material

Refer to Web version on PubMed Central for supplementary material.

Acknowledgments

The authors thank Kirk Cyzmmek for assistance with confocal microscopy and many helpful discussions, Deborah Powell for cryo-SEM sample preparation and analysis, Xiaoqian Ma and Bruce Chase for help and suggestions on FTIR spectra acquisition, and Michael Mackay and Jonathan Seppala for assistance and suggestions on DMA. ^{1}H NMR spectra were obtained with instrumentation supported by NSF CRIF: MU, CHE 0840401. Financial support for this work was provided by the NSF/DMR Biomaterials Program (Jia, Career: 0643226), NSF Integrative Graduate Education & Research Traineeship (IGERT), Center for Neutron Science at the University of Delaware (US Department of Commerce, #70NANB7H6178), and National Institutes of Health (R01 DC008965, P20 RR017716).

References

1. Grieshaber SE, Farran AJE, Lin-Gibson S, Kiick KL, Jia X. Macromolecules. 2009; 42:2532–2541. [PubMed: 19763157]
2. Vrhovski B, Weiss AS. Eur J Biochem. 1998; 258:1–18. [PubMed: 9851686]
3. Hammond TH, Zhou R, Hammond EH, Pawlak A, Gray SD. J Voice. 1997; 11:59–66. [PubMed: 9075177]
4. Wise SG, Weiss AS. Int J Biochem Cell Biol. 2009; 41:494–497. [PubMed: 18468477]
5. Krishna OD, Kiick KL. Biopolymers. 2010; 94:32–48. [PubMed: 20091878]
6. Jia XQ, Kiick KL. Macromol Biosci. 2009; 9:140–156. [PubMed: 19107720]

7. Bellingham CM, Lillie MA, Gosline JM, Wright GM, Starcher BC, Bailey AJ, Woodhouse KA, Keeley FW. Biopolymers. 2003; 70:445–455. [PubMed: 14648756]
8. Simnick AJ, Lim DW, Chow D, Chilkoti A. Polym Rev. 2007; 47:121–154.
9. Klok H-A. J Polym Sci, Part A: Polym Chem. 2005; 43:1–17.
10. Perlin L, MacNeil S, Rimmer S. Soft Matter. 2008; 4:2331–2349.
11. Sreejalekshmi KG, Nair PD. J Biomed Mater Res A. 2011; 96A:477–491. [PubMed: 21171167]
12. Ruoslahti E. Annu Rev Cell Dev Biol. 1996; 12:697–715. [PubMed: 8970741]
13. Shu JY, Tan C, DeGrado WF, Xu T. Biomacromolecules. 2008; 9:2111–2117. [PubMed: 18627200]
14. Jain A, Ashbaugh HS. Biomacromolecules. 2011; 12:2729–2734. [PubMed: 21657254]
15. Sahin E, Kiick KL. Biomacromolecules. 2009; 10:2740–2749. [PubMed: 19743840]
16. Cavanagh, JF.; WJ; Palmer, AG.; Rance, M.; Skelton, NJ. Protein NMR Sp. 2. Elsevier Inc; Burlington, MA: 2007. p. 223-224.
17. Hoult DI. J Magn Reson. 1976; 21:337–347.
18. Chan TR, Hilgraf R, Sharpless KB, Fokin VV. Org Lett. 2004; 6:2853–2855. [PubMed: 15330631]
19. Bax DV, Rodgers UR, Bilek MMM, Weiss AS. J Biol Chem. 2009; 284:28616–28623. [PubMed: 19617625]
20. Hersel U, Dahmen C, Kessler H. Biomaterials. 2003; 24:4385–4415. [PubMed: 12922151]
21. Trabocchi A, Menchi G, Danieli E, Potenza D, Cini N, Bottoncetti A, Raspanti S, Pupi A, Guarna A. Amino Acids. 2010; 38:329–337. [PubMed: 19267182]
22. Zhang H, Aina OH, Lam KS, de Vere White R, Evans C, Henderson P, Lara PN, Wang X, Bassuk JA, Pan C-X. Urol Oncol: Semin Orig Invest. 201010.1016/j.urolonc.2010.06.011
23. Reinhart BR, Lee LL. Cell Tissue Res. 2002; 307:165–172. [PubMed: 11845323]
24. Hautanen A, Gailit J, Mann DM, Ruoslahti E. J Biol Chem. 1989; 264:1437–1442. [PubMed: 2521482]
25. Akiyama SK, Yamada KM. J Biol Chem. 1985; 260:10402–10405. [PubMed: 3161878]
26. Pierschbacher MD, Ruoslahti E. J Biol Chem. 1987; 262:17294–17298. [PubMed: 3693352]
27. Salinas CN, Anseth KS. J Tissue Eng Regener Med. 2008; 2:296–304.
28. Kolb HC, Finn MG, Sharpless KB. Angew Chem Int Edit. 2001; 40:2004–2021.
29. Binder WH, Sachsenhofer R. Macromol Rapid Comm. 2008; 29:952–981.
30. Punna S, Kuzelka J, Wang Q, Finn MG. Angew Chem Int Edit. 2005; 44:2215– 2220.
31. van Dijk M, Nollet ML, Weijers P, Dechesne AC, van Nostrum CF, Hennink WE, Rijkers DTS, Liskamp RMJ. Biomacromolecules. 2008; 9:2834–2843. [PubMed: 18817441]
32. Pedersen DS, Abell A. Eur J Org Chem. 2011; 2011:2399–2411.
33. Horne WS, Yadav MK, Stout CD, Ghadiri MR. J Am Chem Soc. 2004; 126:15366–15367. [PubMed: 15563148]
34. Odian, G. Principles of polymerization. 4. John Wiley & Sons, Inc; Hoboken, NJ: 2004.
35. Farmer RS, Kiick KL. Biomacromolecules. 2005; 6:1531–1539. [PubMed: 15877375]
36. Borders CL, Broadwater JA, Bekeny PA, Salmon JE, Lee AS, Eldridge AM, Pett VB. Protein Sci. 1994; 3:541–548. [PubMed: 8003972]
37. Wishart DS. Prog Nucl Mag Res Sp. 2011; 58:62–87.
38. Wishart DS, Sykes BD, Richards FM. J Mol Bio. 1991; 222:311–333. [PubMed: 1960729]
39. Dalgarno DC, Levine BA, Williams RJP. Bioscience Rep. 1983; 3:443–452.
40. Li LQ, Teller S, Clifton RJ, Jia XQ, Kiick KL. Biomacromolecules. 2011; 12:2302–2310. [PubMed: 21553895]
41. Nowatzki PJ, Tirrell DA. Biomaterials. 2004; 25:1261–1267. [PubMed: 14643600]
42. Aaron BB, Gosline JM. Biopolymers. 1981; 20:1247–1260.
43. Faury G. Pathol Biol. 2001; 49:310–325. [PubMed: 11428167]
44. Lv H, Zhang S, Wang B, Cui S, Yan J. J Controlled Release. 2006; 114:100–109.

45. Schakenraad JM, Busscher HJ, Wildevuur CR, Arends J. J Biomed Mater Res. 1986; 20:773–84. [PubMed: 3722214]
46. McKeehan WL, Ham RG. J Cell Bio. 1976; 71:727–734. [PubMed: 993268]
47. Webb K, Hlady V, Tresco PA. J Biomed Mater Res. 1998; 41:422–430. [PubMed: 9659612]
48. Hatten ME. J Cell Bio. 1981; 89:54–61. [PubMed: 7228900]
49. Mao XL, Peng H, Ling JQ, Friis T, Whittaker AK, Crawford R, Xiao Y. Biomaterials. 2009; 30:6903–6911. [PubMed: 19796804]
50. Yavin E, Yavin Z. J Cell Bio. 1974; 62:540–546. [PubMed: 4609989]
51. Zamir E, Geiger B. J Cell Sci. 2001; 114:3583–3590. [PubMed: 11707510]
52. Anstis GR, Chantikul P, Lawn BR, Marshall DB. J Am Chem Soc. 1981; 64:533– 538.
53. Discher DE, Janmey P, Wang Y-l. Science. 2005; 310:1139–1143. [PubMed: 16293750]
54. Gil ES, Mandal BB, Park SH, Marchant JK, Omenetto FG, Kaplan DL. Biomaterials. 2010; 31:8953–8963. [PubMed: 20801503]
55. Shu XZ, Ghosh K, Liu Y, Palumbo FS, Luo Y, Clark RA, Prestwich GD. J Biomed Mater Res A. 2004; 68A:365–375. [PubMed: 14704979]
56. Mih JD, Sharif AS, Liu F, Marinkovic A, Symer MM, Tschumperlin DJ. PLOS One. 2011; 6:e19929. [PubMed: 21637769]
57. Kim TG, Park TG. Tissue Eng. 2006; 12:221–233. [PubMed: 16548681]
58. Massia SP, Hubbell JA. J Cell Bio. 1991; 114:1089–1100. [PubMed: 1714913]
59. Rowley JA, Mooney DJ. J Biomed Mater Res. 2002; 60:217–223. [PubMed: 11857427]

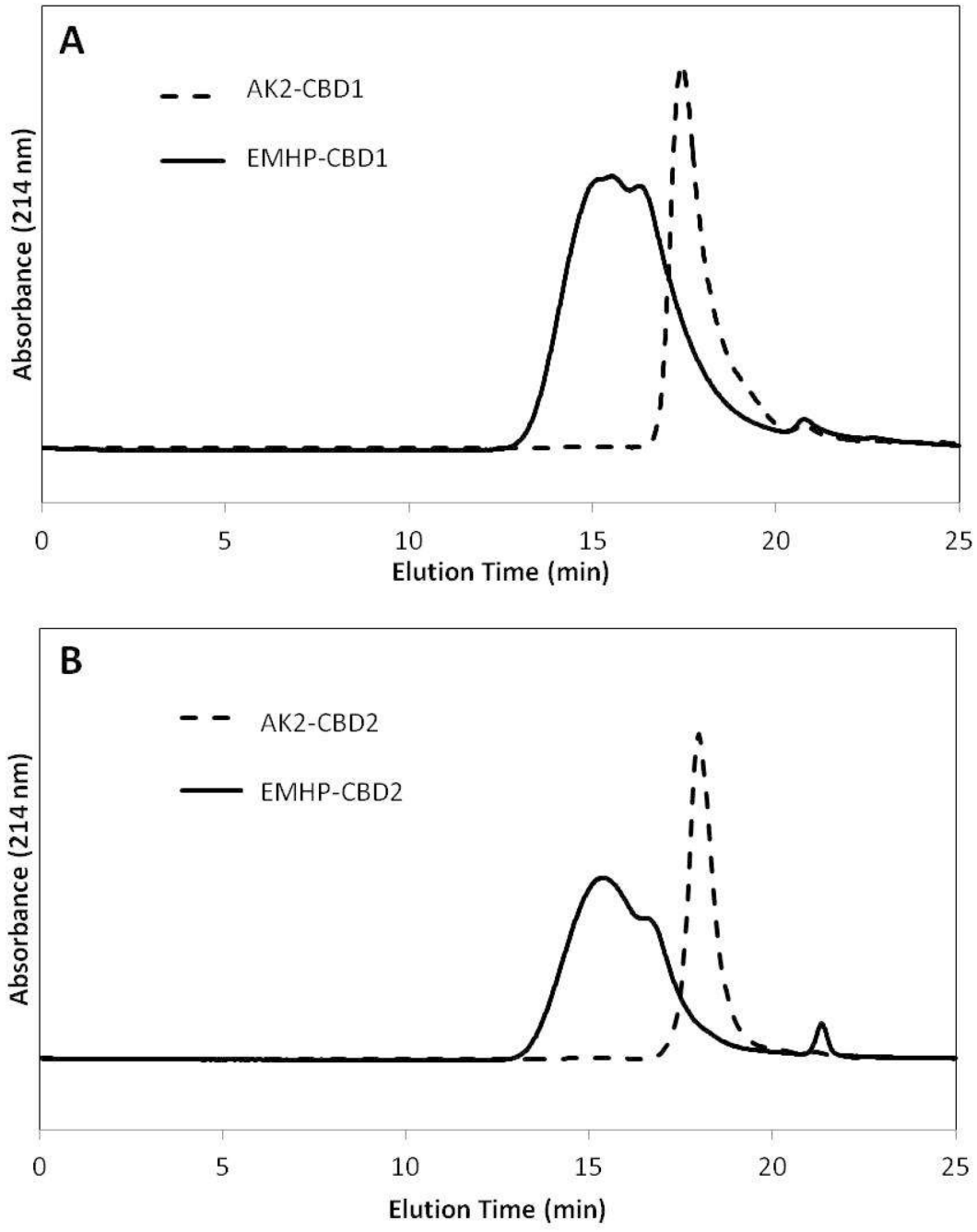

Figure 1.

GPC characterization of the step growth polymerization of AK2-CBD1 (A) and EMHP-CBD1 (B) with N_3-PEG-N_3. Mobile phase: PBS, pH=7.4. Detector: photodiode array (PDA) at 214 nm. Molecular weights calculated by comparison with protein standards.

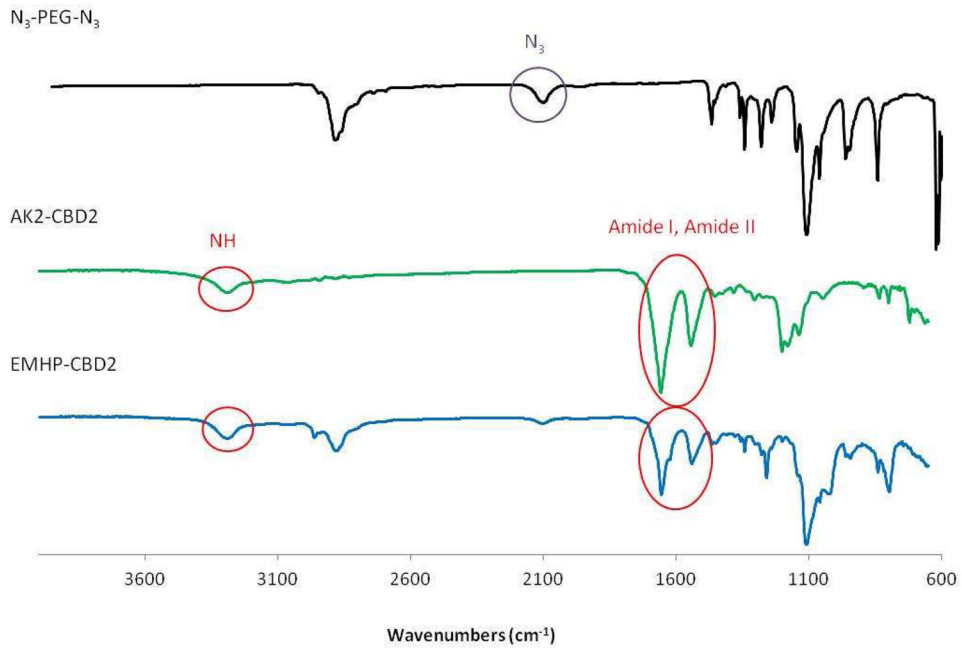

Figure 2.
FTIR spectra of N_3-PEG-N_3, AK2-CBD2 peptide, and EMHP-CBD2.

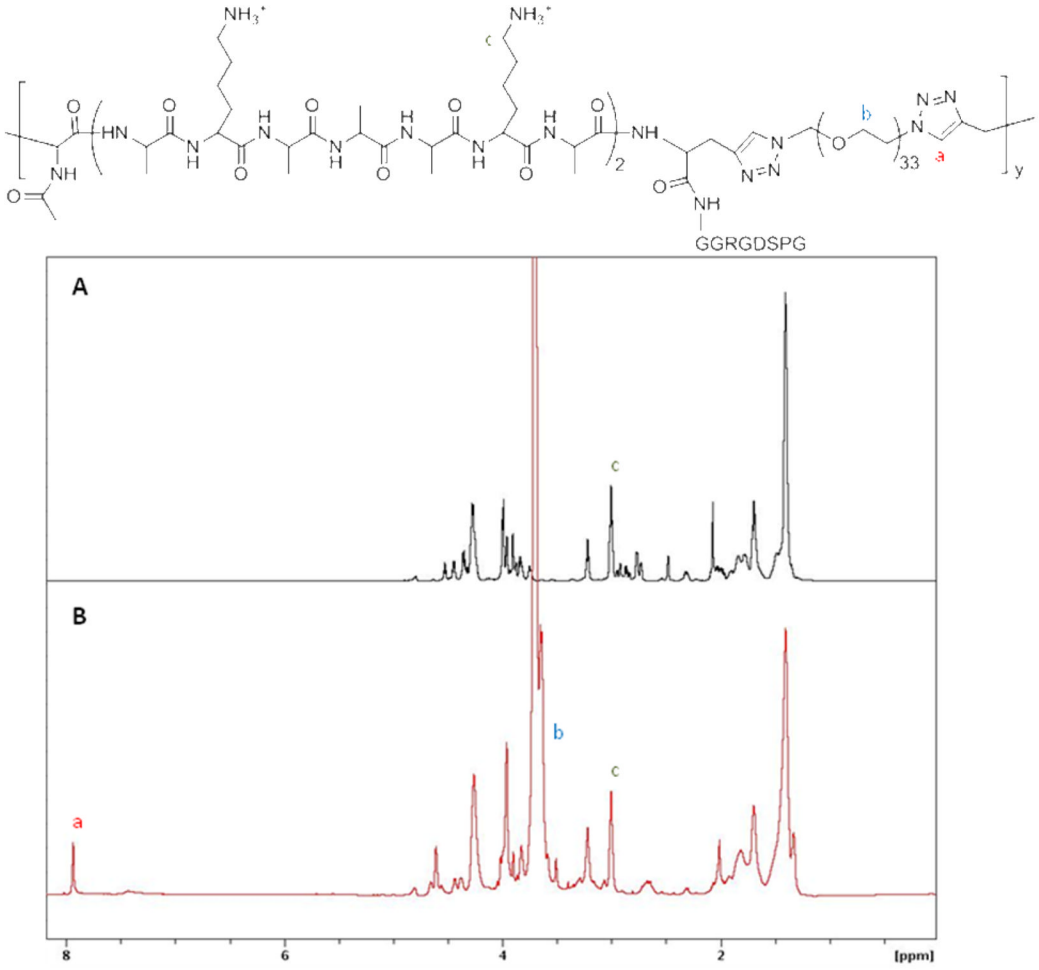

Figure 3.
^{1}H NMR spectra of AK2-CBD2 peptide (A) and EMHP-CBD2 (B) in D_2O with water suppression by presaturation.

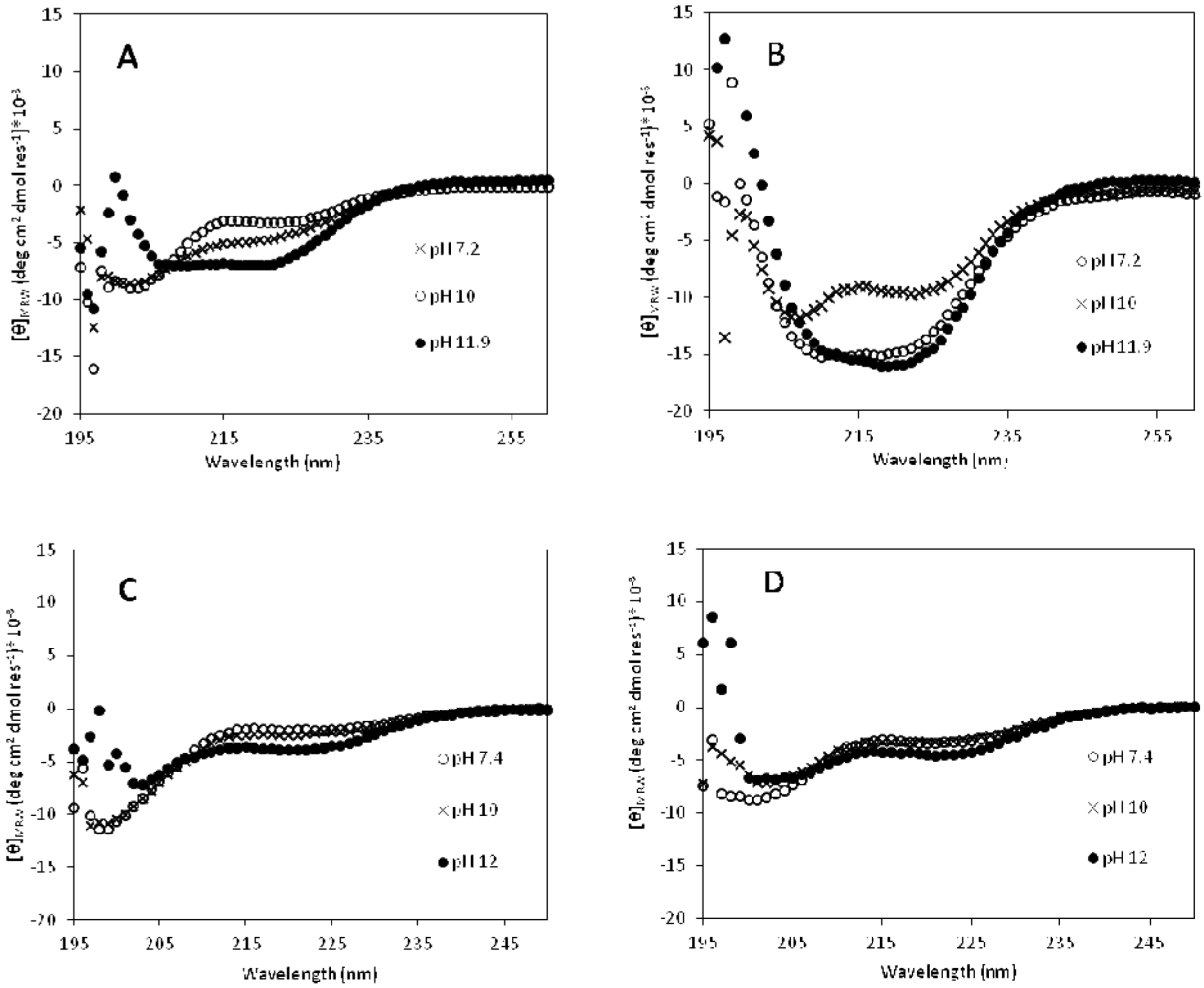

Figure 4.
Circular dichroism spectra of AK2-CDB1 peptide (A), EMHP-CBD1 (B), and AK2- CBD2 (C), and EMHP-CBD2 (D) at pH 7.4, 10, 12. All spectra were measured in PBS at 20 °C.

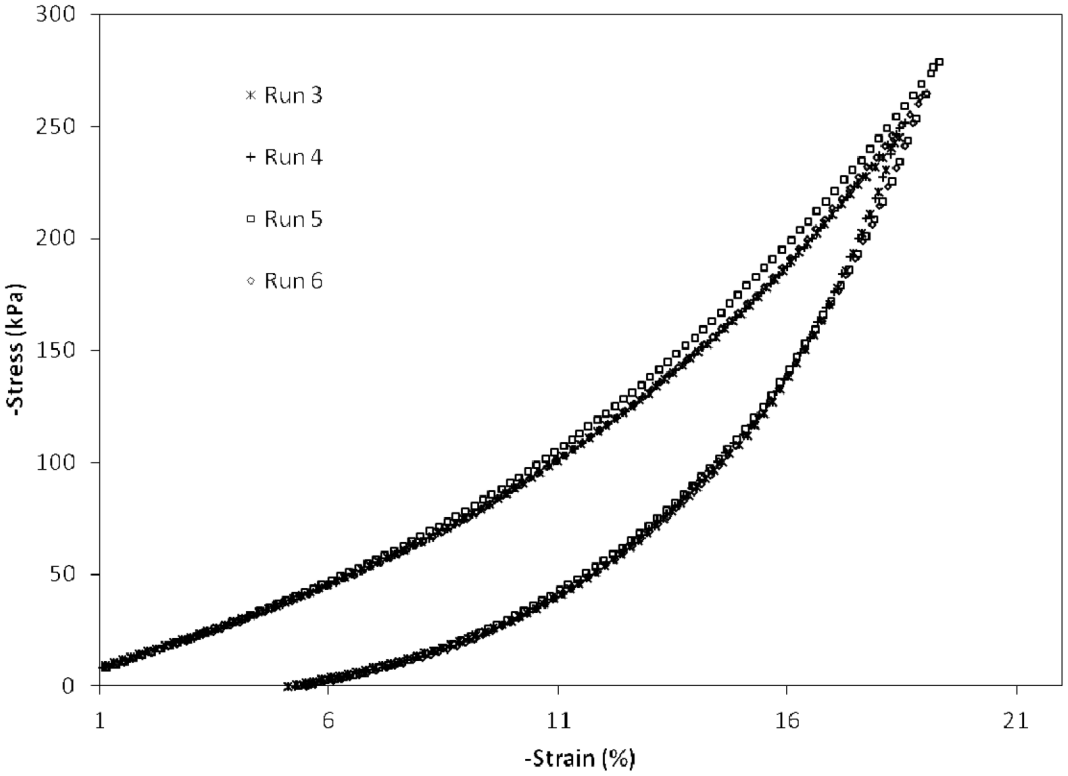

Figure 5.
Representative loading-unloading curves for hydrated xEMHP-CBD2. Samples were allowed to recover for 1 min after each run.

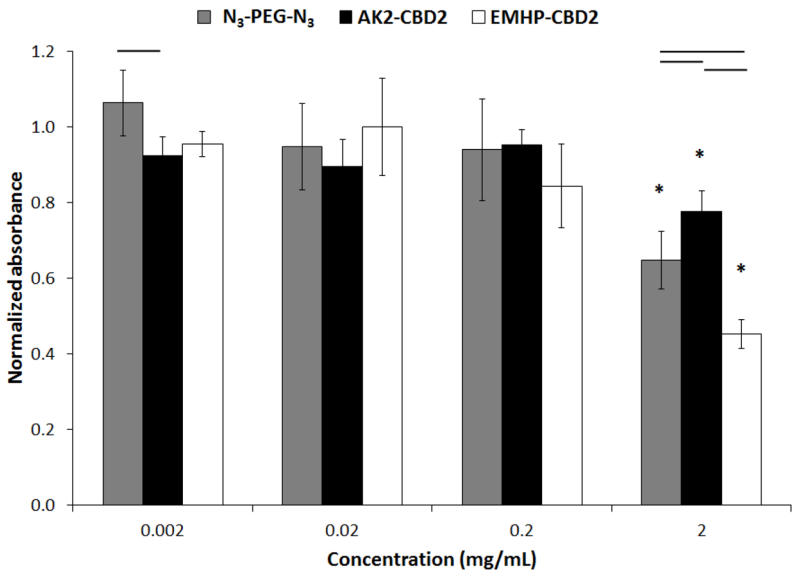

Figure 6.

MTT assay of N_3-PEG-N_3, AK2-CBD2 peptide, and EMHP-CBD2 multiblock at concentrations of 0.002, 0.02, 0.2, and 2 mg/mL using NHDF. An asterisk indicates statistical difference from other concentrations of the same material and a bar indicates statistical difference between two materials at the same concentration when $p \leq 0.02$.

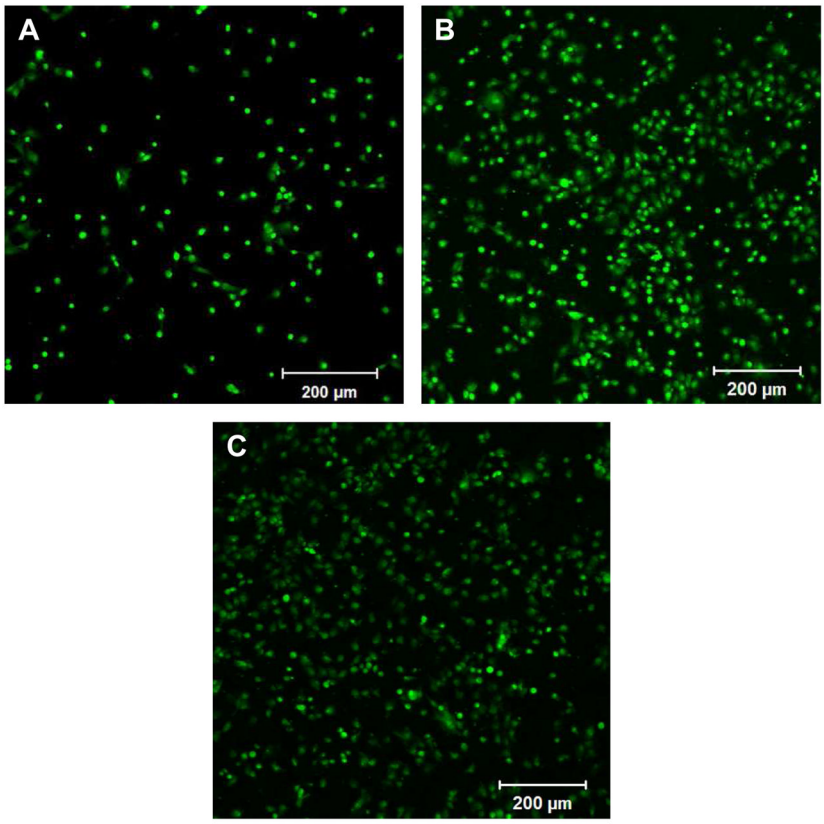

Figure 7.
NHDF attachment on glass (A), xEMHP (B), and xEMHP-CBD2 (C) after 3 h in serum-free media. NHDFs were stained with CellTracker Green prior to cell seeding. Scale bar 200 μm.

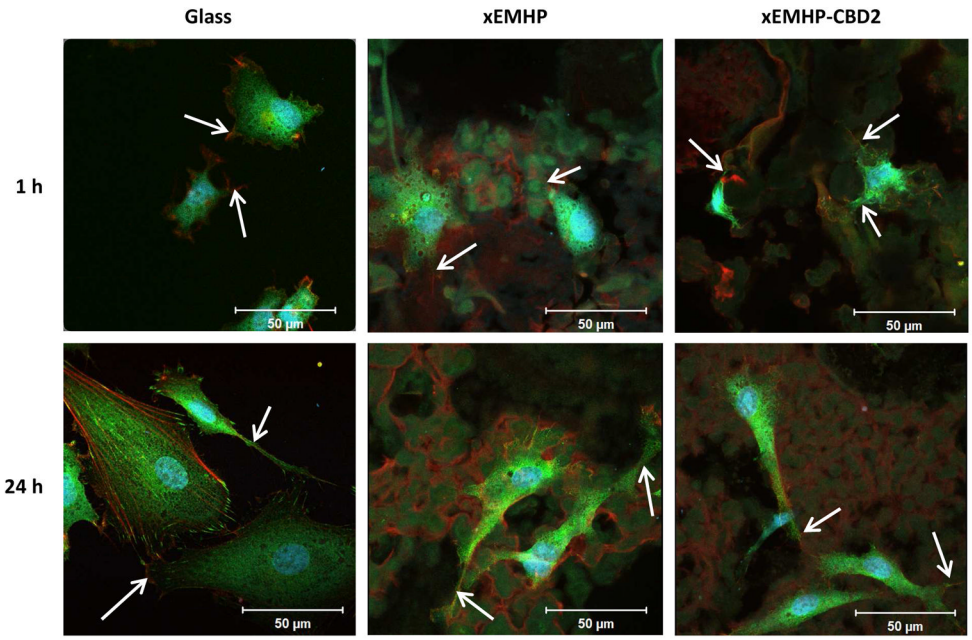

Figure 8.
Cell attachment (NHDFs) on glass, xEMHP, and xEMHP-CBD2 after 1h and 24h. NHDFs were stained with Draq-5 (nuclei, blue), TRITC-phalloidin (F-actin, red), and mouse anti-vinculin (primary antibody) and Alexa 488 anti-mouse (secondary antibody) (vinculin, green).

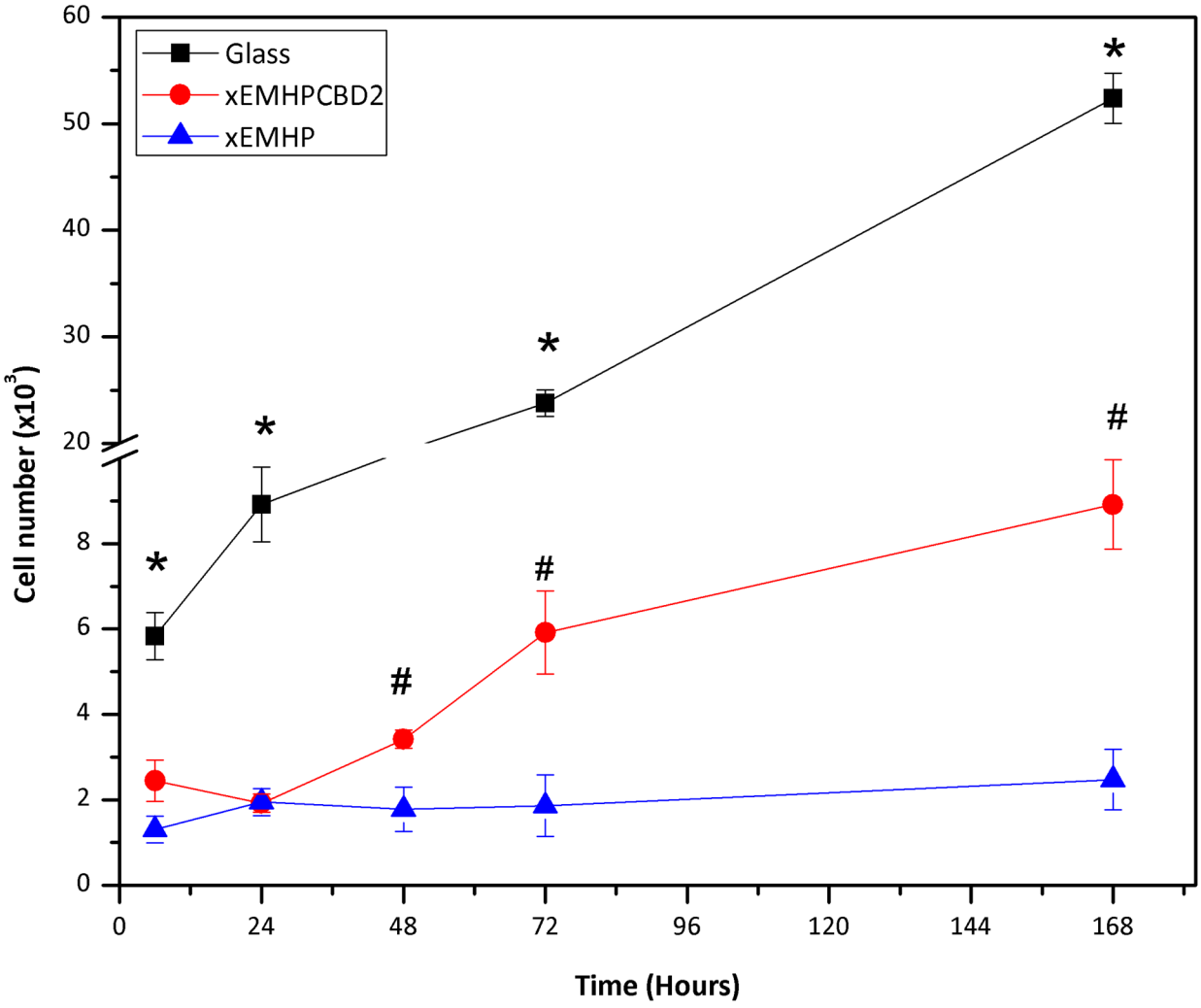

Figure 9.
Proliferation of NHDFs on glass (black squares), xEMHP-CBD2 (red circles) and xEMHP free of CBDs (blue triangles) in serum-free media. Statistical analysis: an asterisk indicates statistical difference between glass and both xEMHPs, and a pound sign indicates statistical difference betwenn xEMHP-CBD2 and xEMHP at a specific time point, with $p \leq 0.01$.

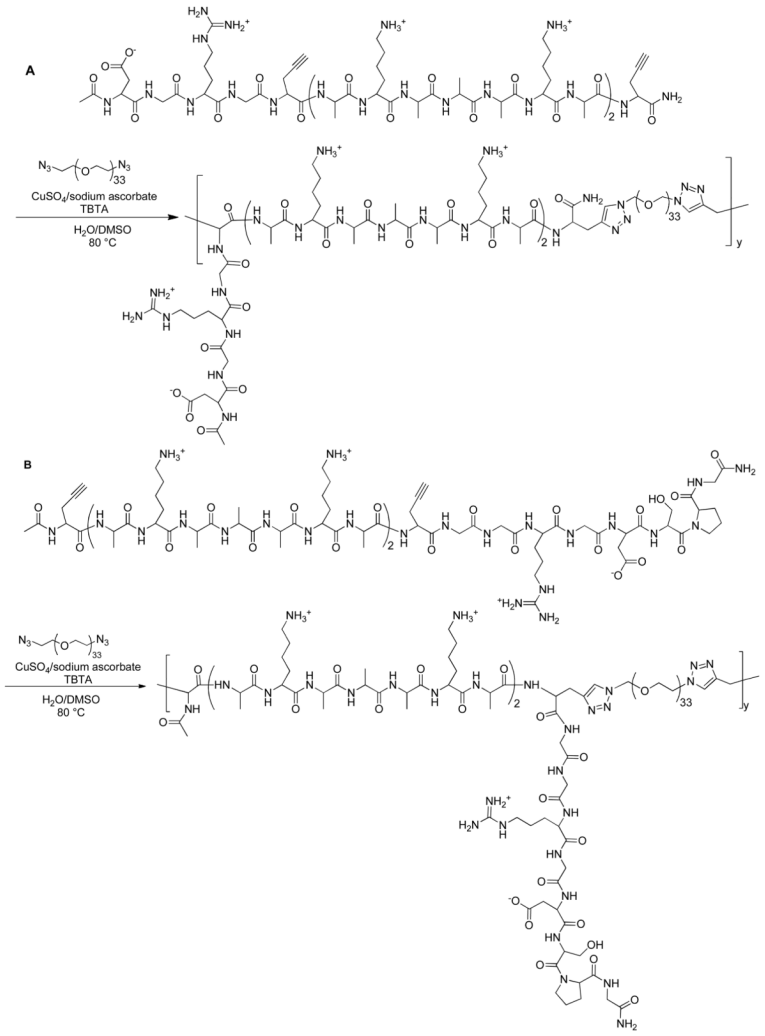

Scheme 1.

Synthesis of EMHP-CBD1 (A) and EMHP-CBD2 (B) by step growth polymerization using azide-functionalized PEG and alkyne-terminated AK2-CBD1 (A) or AK2-CBD2 (B) peptides.

Table 1

Fractional helicity of peptides and EMHPs at pH 7.4, 10, and 12.

Sample ID	Fractional helicity		
	pH 7.4	pH 10	pH 12
AK2-CBD1 peptide	9.3%	6.6%	13.7%
EMHP-CBD1	42.4%	28.3%	46.1%
AK2-CBD2 peptide	3.9%	4.8%	7.8%
EMHP-CBD2	6.6%	6.7%	9.0%